

## Time-Resolved Simultaneous SAXS/WAXS of the Drawing of Polyethylene at the Daresbury SRS

D. J. Hughes,<sup>a</sup> A. Mahendrasingam,<sup>a</sup> E. L. Heeley,<sup>a</sup> W. B. Oatway,<sup>a</sup>  
C. Martin,<sup>a</sup> E. Towns-Andrews<sup>b</sup> and W. Fuller<sup>a</sup>

<sup>a</sup>Department of Physics, Keele University, Staffordshire ST5 5BG, UK, and <sup>b</sup>Daresbury Laboratory, Warrington WA4 4AD, UK

(Received 4 December 1995; accepted 2 January 1996)

A system has been developed which represents a significant advance in the quality and extent of small- and wide-angle X-ray scattering data (SAXS and WAXS) that can be recorded simultaneously with strain data during the drawing and annealing of polymer materials. WAXS data are recorded using a Photonic Science charge-coupled-device area detector and SAXS data using a gas-filled multiwire area detector. Strain data, for the region of the specimen from which the SAXS/WAXS data are collected, are calculated from an accurately synchronized continuously recorded video image of the specimen. The system allows X-ray and video image data to be collected as a series of frames with essentially no 'dead-time' between frames. The data are fully two-dimensional and can be collected for a wide range of  $d$  spacings. The use of this system to investigate the stress-induced orientation and phase changes during the drawing of a range of grades of commercially available polyethylene is described.

**Keywords:** SAXS; WAXS; X-ray fibre diffraction; polyethylene; time-resolved studies.

### 1. Introduction

X-ray fibre diffraction is the favoured technique for the investigation of the structural changes induced in organic polymers during drawing and annealing. Wide-angle X-ray scattering (WAXS) data are typically collected in the range  $\sim 50$  to  $1 \text{ \AA}$ , whilst useful small-angle X-ray scattering (SAXS) data are commonly in the range  $\sim 500$  to  $50 \text{ \AA}$ . The advent of high-brilliance synchrotron radiation sources such as the Daresbury SRS allowed rapid time-resolved separate SAXS and WAXS experiments to be performed (Faruqi, Huxley, Simmons & Bond, 1991; Blundell *et al.*, 1994; Mahendrasingam *et al.*, 1995). However, there are always difficulties in correlating data recorded in separate SAXS and WAXS experiments. These may be due to different drawing behaviours of different samples of the same material in addition to differences in a variety of experimental parameters which in practice are difficult to control precisely. Various strategies have been adopted in order to record SAXS and WAXS data simultaneously (Wutz, Bark, Cronauer, Dohrmann & Zachmann, 1995; Bras *et al.*, 1993; Laggner & Mio, 1992). The only practical solution that provides adequate time resolution, however, is to use two electronic detectors. In order to collect the full two-dimensional diffraction data from an oriented polymer, it is crucial that they are both genuinely area detectors.

Recently, a simultaneous SAXS/WAXS facility has been developed involving the use of two gas-filled multiwire area detectors (Bras *et al.*, 1995). This system has proved a useful tool for the study of polymer deformation (Butler *et al.*, 1995), though the use of a gas-filled multiwire detector

for the collection of WAXS data suffers from fundamental limitations. These are:

- (i) parallax problems caused by the active depth of the detector;
- (ii) the maximum global count rate of the detector necessitates attenuation of the pattern, which results in a reduced count rate in the data;
- (iii) problems with positioning the detector for optimum WAXS collection due to its physical size.

The SAXS/WAXS system proposed here also uses a multiwire area detector to collect SAXS data, but uses a charge-coupled-device (CCD)-based area detector to collect WAXS data. This novel configuration allows simultaneous SAXS/WAXS data to be gathered at rates limited by the maximum count rate of the SAXS detector.

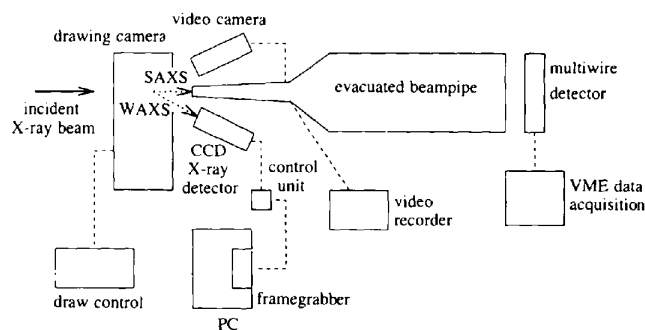


**Figure 1**  
Schematic representation of the experimental arrangement on beamline 16.1.

## 2. Experimental technique

The SAXS/WAXS facility described here has been designed to be portable so that with only minor modifications it can be used on a variety of beamlines. Here it has been used in

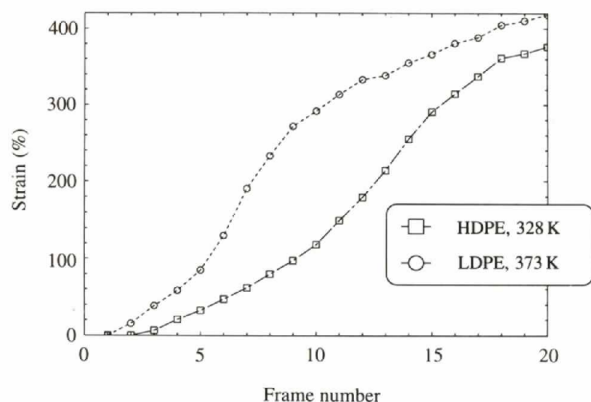


**Figure 2**  
Plots showing the variation of strain during the drawing of HDPE and LDPE.

experiments performed on beamline 16.1 of the Daresbury SRS (Bliss *et al.*, 1995), which has proved to be the most successful station for recording SAXS/WAXS data. The data described in this paper were all collected using this beamline.

The camera was constructed in the Keele Physics Department workshop. It allows drawing and annealing of synthetic polymers at temperatures from ambient to 623 K and draw rates up to  $72\,000\% \text{ min}^{-1}$  (Mahendrasingam *et al.*, 1992). In previous studies this camera has been used to collect separate SAXS and WAXS data sets. The camera consists of a  $150 \times 150 \times 150 \text{ mm}$  oven with two stepper-motor-driven jaws, which allow uniaxial drawing of samples. The SAXS and WAXS exit window is a sheet of thin aluminium foil ( $\approx 15 \mu\text{m}$ ). However, to eliminate the appearance of strong aluminium reflections from the WAXS pattern, a circular glass cover slip ( $13 \text{ mm}$  diameter,  $\sim 10 \mu\text{m}$  thick) was placed over a hole that was cut in the middle of the aluminium window. The centre of the glass cover slip was then made to coincide with the main beam position so that the SAXS passes wholly through the glass cover slip. Since the main beam no longer passed

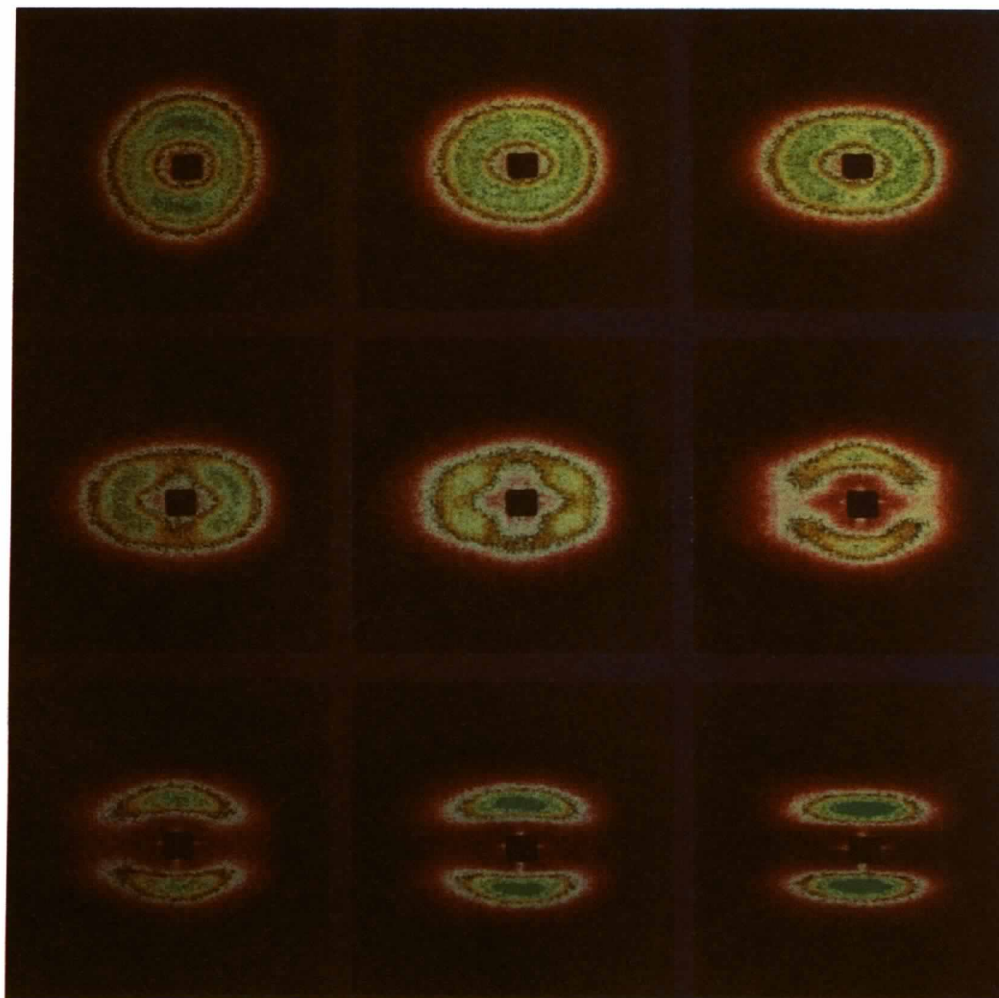


**Figure 3**  
Selection of SAXS frames from the drawing of LDPE. Frame numbers correspond to those shown in the grid.

through the aluminium window, there were no aluminium reflections in the WAXS pattern.

The gas-filled multiwire area detector that was used to collect SAXS data had an active area of  $20 \times 20$  cm, and was controlled by a VME-based data-acquisition system (Helsby *et al.*, 1994). This detector provides a theoretical minimum time resolution of  $10 \mu\text{s}$ . However, in practice, for these experiments, because of limitations in the global count rate of the detector, exposure times of a few seconds were needed to achieve acceptable quality data. As a result of the count rate limitations the SAXS pattern was substantially attenuated before falling on the detector. An evacuated chamber, specifically modified for these studies by extending the entrance cone, was positioned between the SAXS detector and the exit point from the drawing camera to minimize scattering by air.

The Photonic Science CCD-based area detector used to collect the WAXS data had an X-ray photon detection system which consisted of a thin gadolinium oxysulfide scintillator fibre optically coupled to a low-light-level CCD image intensifier. The detector had an active area of  $92 \times 69$  mm on the imaging phosphor, giving an effective pixel resolution of  $\sim 120 \mu\text{m}$ . The full width at half maximum (FWHM) of the point spread function (PSF) is no more than a few pixels, which makes this detector ideal for the

collection of X-ray fibre diffraction data. It is possible to show that the detector quantum efficiency (DQE) of the Photonic Science CCD detector system is  $\sim 0.7$ , which is comparable to that of similar electronic detectors (Gao, Li, Rousseau, Linliu & Chu, 1993). The maximum count rate that the detector can measure is determined by the full-well capacity of the CCD. Adjusting the variable intensifier gain ensures that CCD saturation does not occur.

The detector was positioned close to the drawing camera, thereby reducing air scatter to a minimum. In the experiments detailed in the following section, the face of the detector was positioned at an angle of  $25^\circ$  from normal to the beam. This enabled the maximum amount of WAXS data to be collected whilst still allowing SAXS data to pass unobstructed for collection at the multiwire detector. Subsequent correction of WAXS data to a flat geometry for detailed analysis is relatively simple.

Output from the WAXS detector is in the form of a standard CCIR video signal which gives a frame rate of  $25 \text{ s}^{-1}$ . A Synoptics i860-based video framegrabber is controlled by an IBM compatible 486DX2-66 PC. The framegrabber has 32 MB of on-board memory and is able to digitize successive 40 ms frames and store them directly into memory with no data loss using 8-bit digitization of the video signal.

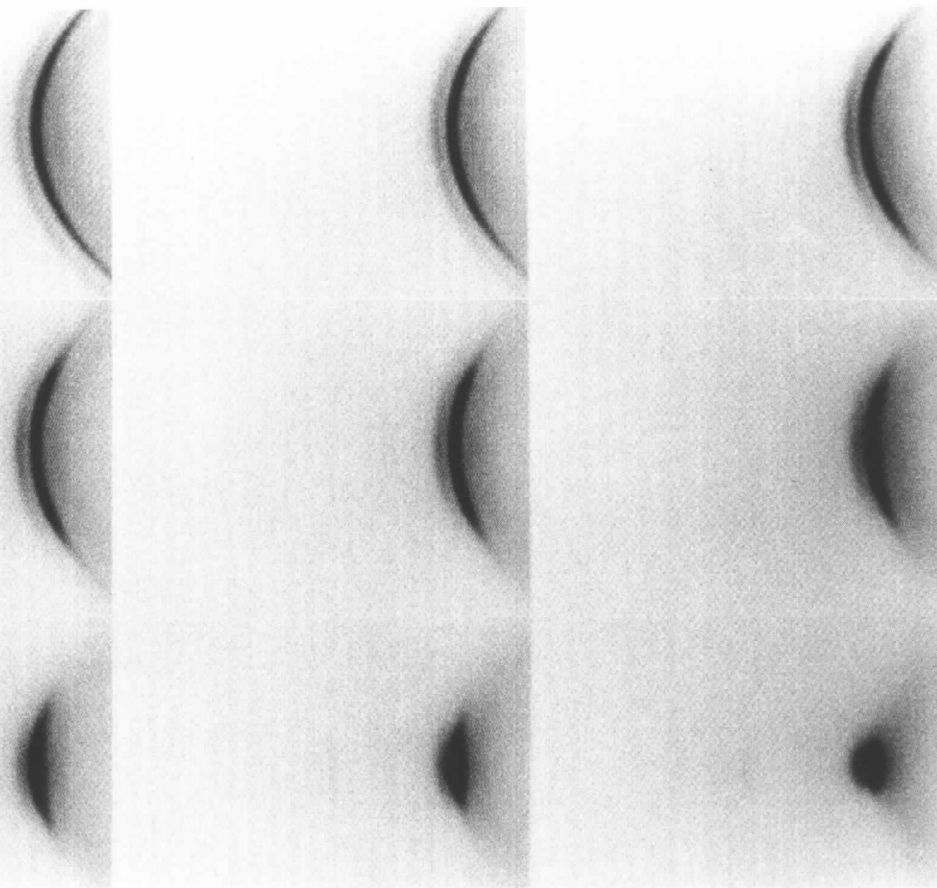


**Figure 4**

Selection of WAXS frames from the drawing of LDPE collected simultaneously with the SAXS data shown in Fig. 3.

The framegrabber software has been developed to allow flexibility of data-collection methodologies so that many diverse experiments utilizing this system are possible. Although framegrabbing has to be performed under MSDOS, the PC has also been installed with a Unix environment (Linux 1.1.92) with an X-windows graphical interface and software to allow rapid display and interrogation of the experimental data. Short-term data storage is provided by an external 1.4 GB hard disc with a fast SCSI disc controller. Long-term data backup is *via* a DAT tape drive.

To enable the SAXS/WAXS data to be correlated with a particular sample strain, a video camera was mounted outside the drawing camera and was fitted with a close-up lens. Video data were recorded to video tape using a standard VCR during the draw. It was then possible to use the framegrabber system at a later date to obtain individual physical draw frames that correspond to the SAXS/WAXS data. Strain information at the position on the specimen from where the SAXS/WAXS data were recorded can then be calculated from the position of reference lines marked on the sample before drawing.

Fig. 1 is a schematic representation of the experimental arrangement on beamline 16.1 at the Daresbury SRS.

### 3. Results

Samples of commercial low-density polyethylene (LDPE) and high-density polyethylene (HDPE) were purchased from Goodfellow in sheets of 1 mm thickness. Samples 10 mm wide and 20 mm long were cut from these sheets and were mounted in the metal jaws within the drawing camera. We have performed experiments at different draw rates and temperatures. Two examples of typical experiments are given below to illustrate the capabilities of this system. The local strain variation at the beam position for both experiments is shown in Fig. 2.

#### 3.1. Drawing of LDPE

A sample of LDPE was drawn at 373 K. The nominal draw rate was  $100\% \text{ min}^{-1}$ . However, as can be seen from Fig. 2, the local draw rate at the point in the specimen from which the WAXS and SAXS data were collected varies widely during the experiment. SAXS data were collected in the form of 20 consecutive 10 s frames. Fig. 3 shows selected SAXS frames that highlight the principal changes in the small-angle pattern during the draw.

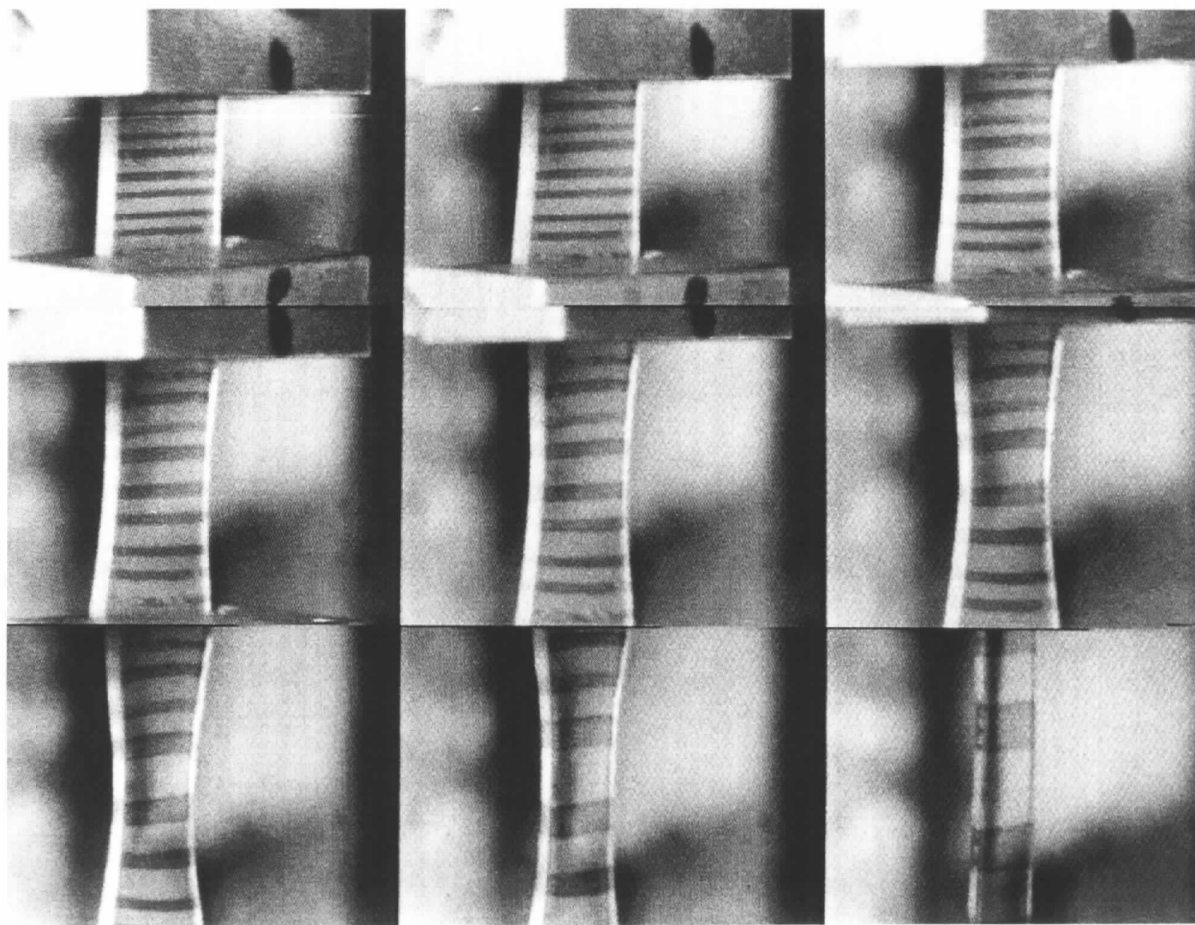


**Figure 5**

Selection of draw frames collected simultaneously with the SAXS/WAXS data in Figs. 3 and 4.



Corresponding WAXS patterns were collected simultaneously and are shown in Fig. 4. Fig. 5 shows the changes in the dimensions of the specimen during the draw; frames correspond to those in Figs. 3 and 4.

In the initial WAXS frame, two rings of intensity are clearly visible. These may be indexed as reflections from the (110) and (200) planes of the orthorhombic form of polyethylene. Other reflections associated with smaller  $d$  spacings are observed, though these are not obvious in Fig. 4. It is apparent from frame 1 in Fig. 4 that some pre-orientation exists in this sample in the direction of the intended draw. The initial SAXS frame also shows evidence of this pre-orientation. However, the overall feature is that of a predominantly isotropic ring corresponding to a spherulitic structure with a lamellar long spacing of  $\sim 190$  Å.

From the sequence of WAXS patterns it is apparent that increasing strain results in increasing equatorial orientation of both the (110) and (200) reflections, thus indicating  $c$ -axis orientation parallel to the direction of draw.

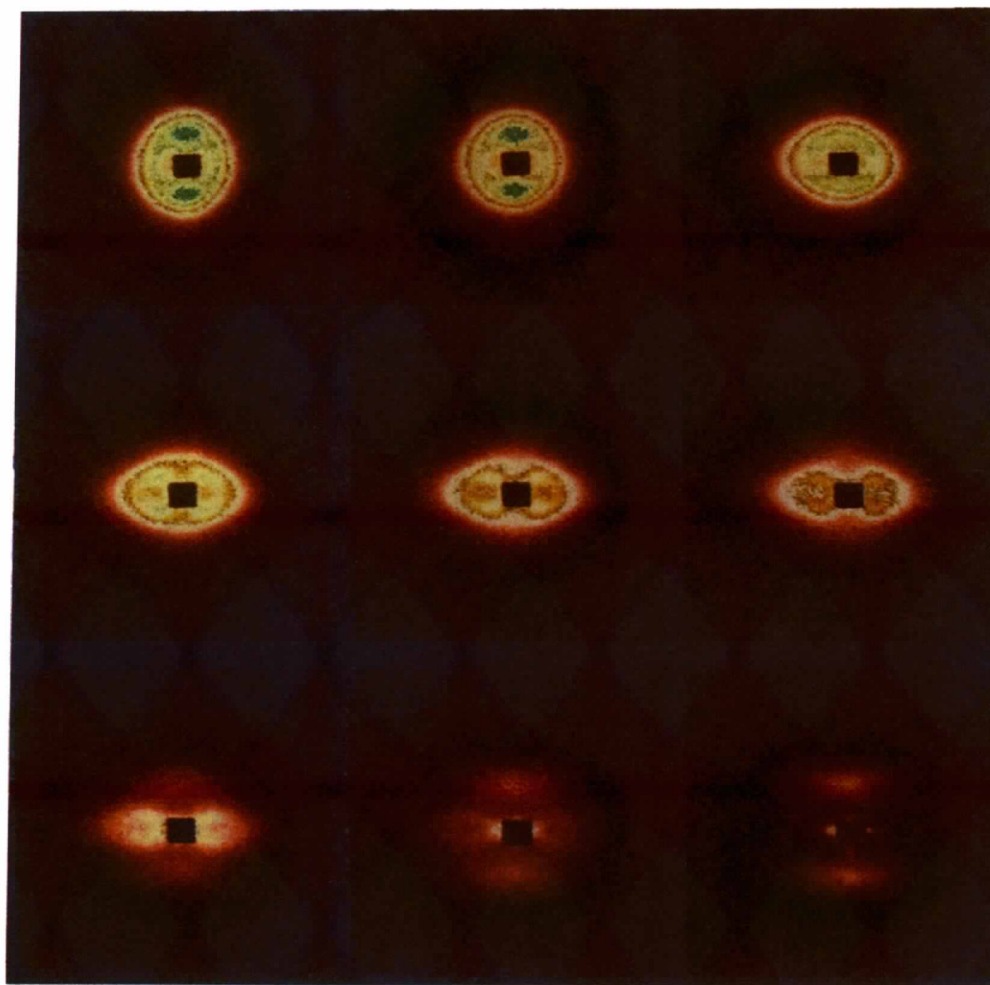
The SAXS patterns are rather more striking, and show the distortion of the lamellae into a V-shaped structure

(Wilke & Bratrich, 1991) revealed by a four-point pattern (frame 5) at a draw ratio of 2:1. This is followed by destruction of lamellae and transition to a fibrillar structure (frame 20) with a long period of  $\sim 215$  Å.

### 3.2. Drawing of HDPE

A sample of HDPE was drawn at 328 K at a rate of  $100\% \text{ min}^{-1}$ . A total of twenty 10 s frames were collected. Selected SAXS frames are shown in Fig. 6 and the corresponding WAXS patterns are displayed in Fig. 7. The change in the dimensions of the specimen during the draw is shown in Fig. 8.

The initial SAXS/WAXS patterns are similar to those obtained from the low-density sample. The first WAXS frame in Fig. 7 clearly shows both the (110) and (200) reflections, though other reflections are more easily observed due to a higher degree of crystallinity in this sample. The initial SAXS pattern loosely resembles an isotropic ring indicating a lamellar long period of  $\sim 255$  Å, but the increased meridional intensity implies some pre-orientation in the intended draw direction.



Frame number

1	3	5
7	8	9
11	13	20

**Figure 6** Selection of SAXS frames from the drawing of HDPE. Frame numbers correspond to those shown in the grid.

It is clear from the WAXS data that the progression of orientation is rather different to that of the low-density sample. At a strain of  $\sim 50\%$  (frame 7), the (110) reflection is clearly split into two components whilst the (200) reflection is equatorial. This is indicative of a tilted crystallite orientation (Vickers & Fischer, 1995). As the strain increases, the preferred orientation becomes one in which the crystallites are aligned with their  $c$  axis parallel to the draw direction. Another interesting feature is the partial temporary stress-induced orthorhombic-to-monoclinic phase change, observed at intermediate strains (Hay & Keller, 1970). In frames 7 to 13 an extra reflection can be seen inside the orthorhombic (110) reflection. This corresponds to the (001) reflection of the monoclinic phase of polyethylene, though the orthorhombic phase is still clearly predominant. The SAXS data are similar to those in the previous experiment, though the final fibrillar structure ( $\sim 175 \text{ \AA}$ ) is less pronounced due to the lower draw temperature.

#### 4. Conclusions

The system that we have developed for the collection of time-resolved simultaneous SAXS/WAXS data has proved

to be a very useful tool for the study of the behaviour of organic polymers during drawing and annealing. The quality of the data allows in-depth analysis to be performed on both the SAXS and WAXS data. One of the major advantages in using a CCD-based detector, such as the Photonic Science detector, is its portability. Using an experimental arrangement very similar to that described above, it has proved possible to perform exploratory SAXS/WAXS experiments on beamlines 2.1 and 8.2 at the Daresbury SRS.

We are currently investigating the possibility of using a second CCD-based area detector to collect the SAXS data. An advanced set-up such as this would allow a dramatically reduced minimum time resolution for SAXS/WAXS experiments of the type described in this paper, which is currently determined by the limitations of the multiwire SAXS detector.

The use of the CCD-based area detector for the collection of rapid WAXS data is indicative of the growing use of CCD technology for X-ray imaging (Clarke, Lowe, MacHarrie, Brizard & Rodricks, 1992). CCD-based detectors can offer rapid readout at high count rates with a good spatial resolution. Future CCD chip development is towards

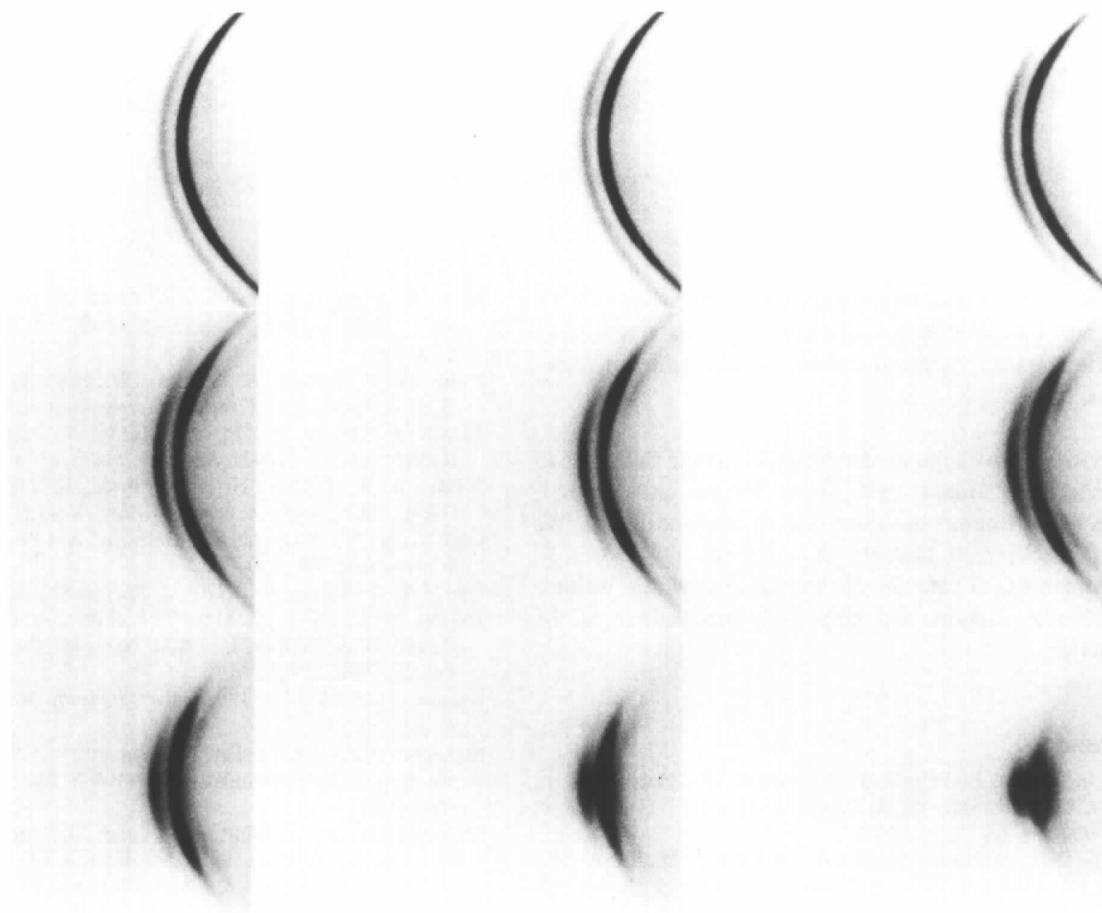


**Figure 7**

Selection of WAXS frames from the drawing of HDPE collected simultaneously with the SAXS data shown in Fig. 6.

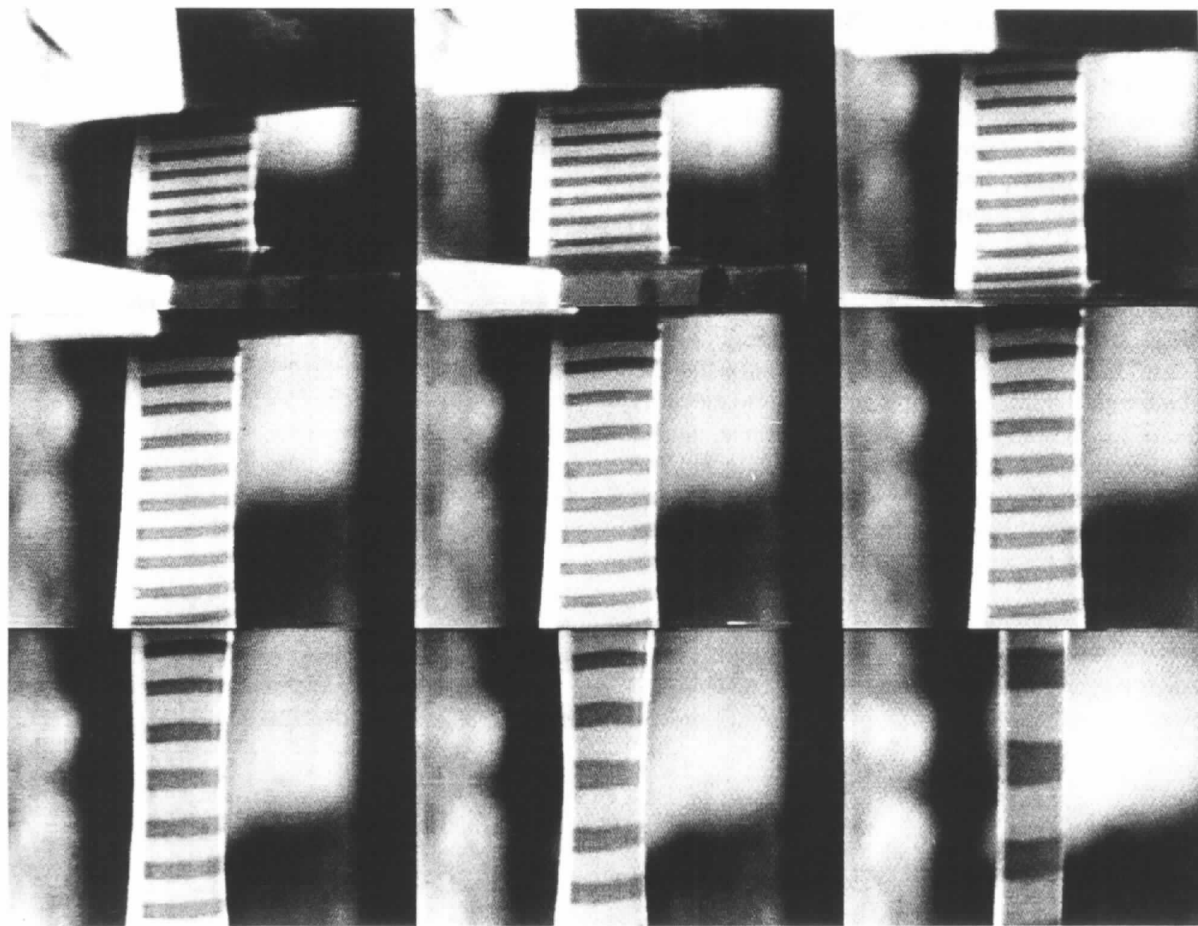


**Figure 8**  
Selection of draw frames collected simultaneously with the SAXS/WAXS data shown in Figs. 6 and 7.

larger pixel arrays and faster readout speeds, making CCD-based detectors even more suitable to high flux synchrotron experiments than currently available alternative detector designs.

This work was supported by EPSRC grant GR/J/86643 to WF, AM, J. Bordas and ET-A. We are grateful to J. Bordas for advice on beamline and instrument design. We thank D. Bowyer, M. Daniels, M. G. Davies, G. Dudley, E. J. T. Greasley, G. Marsh, H. Moors and M. P. Wallace for technical support and help with preparation of the manuscript.

## References

- Bliss, N., Bordas, J., Fell, B. D., Harris, N. W., Helsby, W. I., Mant, G. R., Smith, W. & Towns-Andrews, E. (1995). *Rev. Sci. Instrum.* **66**, 1311–1313.
- Blundell, D. J., Mahendrasingam, A., McKerron, D., Turner, A., Rule, R., Oldman, R. J. & Fuller, W. (1994). *Polymer*, **35**, 3875–3882.
- Bras, W., Derbyshire, G. E., Ryan, A. J., Mant, G. R., Manning, P., Cameron, R. E. & Mormann, W. (1993). *J. Phys. (Paris)*, **3(8)**, 447–450.
- Bras, W., Mant, G. R., Derbyshire, G. E., O’Kane, W. J., Helsby, W. I., Hall, C. J. & Ryan, A. J. (1995). *J. Synchrotron Rad.* **2**, 87–92.
- Butler, M. F., Donald, A. M., Bras, W., Mant, G. R., Derbyshire, G. E. & Ryan, A. J. (1995). *Macromolecules*, **28**, 6383–6393.
- Clarke, R., Lowe, W. P., MacHarrie, R. A., Brizard, C. & Rodricks, B. G. (1992). *Rev. Sci. Instrum.* **63**, 784–789.
- Faruqi, A. R., Huxley, H. E., Simmons, R. M. & Bond, C. C. (1991). *Nucl. Instrum. Methods Phys. Res. A*, **310**, 359–361.
- Gao, T., Li, Y., Rousseau, J., Linliu, K. & Chu, B. (1993). *Rev. Sci. Instrum.* **64**, 390–396.
- Hay, I. L. & Keller, A. (1970). *J. Polym. Sci. C*, **30**, 289–296.
- Helsby, W. I., Berry, A., Hall, C. J., Jones, A. O., Lewis, R. A., Parker, B. & Sumner, I. (1994). *Nucl. Instrum. Methods Phys. Res. A*, **348**, 329–333.
- Laggner, P. & Mio, H. (1992). *Nucl. Instrum. Methods Phys. Res. A*, **323**, 86–90.
- Mahendrasingam, A., Fuller, W., Forsyth, V. T., Oldman, R. J., MacKerron, D. & Blundell, D. J. (1992). *Rev. Sci. Instrum.* **63**, 1087–1090.
- Mahendrasingam, A., Martin, C., Jaber, A., Hughes, D., Fuller, W., Rule, R., Oldman, R. J., MacKerron, D. & Blundell, D. J. (1995). *Nucl. Instrum. Methods Phys. Res. B*, **97**, 238–241.
- Vickers, M. E. & Fischer, H. (1995). *Polymer*, **36**, 2667–2670.
- Wilke, W. & Bratrich, M. (1991). *J. Appl. Cryst.* **24**, 645–650.
- Wutz, C., Bark, M., Cronauer, J., Dohrmann, R. & Zachmann, H. G. (1995). *Rev. Sci. Instrum.* **66**, 1303–1307.